



Hadronic Gamma Rays from Supernova Remnants

I. V. MOSKALENKO^{1,2}, T. A. PORTER³, M. A. MALKOV⁴, P. H. DIAMOND⁴

¹*Hansen Experimental Physics Laboratory, Stanford University, Stanford, CA 94305, U.S.A.*

²*Kavli Institute for Particle Astrophysics and Cosmology, Stanford University, CA 94309, U.S.A.*

³*Santa Cruz Institute for Particle Physics, University of California, Santa Cruz, CA 95064, U.S.A.*

⁴*University of California at San Diego, La Jolla, CA 92093, U.S.A.*

imos@stanford.edu

Abstract: A gas cloud near a supernova remnant (SNR) provides a target for pp -collisions leading to subsequent γ -ray emission through π^0 -decay. The assumption of a power-law ambient spectrum of accelerated particles with index near -2 is usually built into models predicting the spectra of very-high energy (VHE) γ -ray emission from SNRs. However, if the gas cloud is located at some distance from the SNR shock, this assumption is not necessarily correct. In this case, the particles which interact with the cloud are those leaking from the shock and their spectrum is approximately monoenergetic with the injection energy gradually decreasing as the SNR ages. In the GLAST energy range the γ -ray spectrum resulting from particle interactions with the gas cloud will be flatter than expected, with the cutoff defined by the pion momentum distribution in the laboratory frame. We evaluate the flux of particles escaping from a SNR shock and apply the results to the VHE diffuse emission detected by the HESS at the Galactic centre.

Introduction

SNRs are believed to be the primary sources of cosmic rays (CR) in the Galaxy. Observations of X-ray [12] and γ -ray emission [3, 4] from SNR shocks reveal the presence of energetic particles, thus testifying to efficient acceleration processes. Acceleration of particles in collisionless shocks is a matter of intensive research in conjunction with the problem of CR origin [7, 6, 11]. Current models include nonlinear effects (e.g., [5]) and treat particle acceleration using hydrodynamic codes (e.g., [9]). The predicted spectrum of accelerated particles has a power-law form in rigidity with index which may slightly vary around -2 .

The VHE γ -ray emission from shell-type SNRs has been modelled using leptonic (inverse Compton – IC) and hadronic (π^0 -decay) scenarios. The leptonic scenario fits the broad-band spectrum of a SNR assuming a pool of accelerated electrons IC scattering off the interstellar radiation field producing VHE γ -rays while the magnetic field and electron spectrum cut-off are tuned to fit the radio and X-ray data (e.g., [13, 18]). The hadronic model

fits the VHE γ -ray spectrum assuming a beam of accelerated protons hits a target, such as a nearby molecular cloud [1, 14]. The latter, if definitively proven, would be the first experimental evidence of proton acceleration in SNRs.

The assumption of a power-law ambient spectrum of accelerated particles with index near -2 is usually built into the models predicting the spectra of VHE γ -ray emission from SNRs. However, if a molecular cloud is located at some distance from the shock, the particles which interact with the cloud are those leaking from the shock and their spectrum is different [10]. In a toy model, the shock accelerates particles until the highest possible energy is reached. At this point the shock cannot confine the particles any longer and they escape into the interstellar medium (ISM). The energy spectrum of these particles will be monoenergetic with the injection energy gradually decreasing as the SNR ages. The γ -ray spectrum resulting from the particles interacting with a gas cloud will be essentially flatter than expected. The diffuse emission detected at the Galactic centre by the HESS [2] may be of this sort.

Particle acceleration in SNR shock

We use the steady-state diffusion-convection equation

$$u \frac{\partial f}{\partial x} + \kappa(p) \frac{\partial^2 f}{\partial x^2} = \frac{1}{3} \frac{du}{dx} p \frac{\partial f}{\partial p}, \quad (1)$$

where $f(x, p)$ is the isotropic (in the local fluid frame) part of the particle distribution, and p is the particle momentum in mc units. We use a planar geometry and assume that the gaseous discontinuity (sub-shock) is located at $x = 0$ while the shock propagates in the positive x -direction. The flow velocity in the shock frame can be represented as $V(x) = -u(x)$ where the (positive) flow speed $u(x)$ jumps from $u_2 \equiv u(0-)$ downstream to $u_0 \equiv u(0+) > u_2$ across the sub-shock and then gradually increases up to $u_1 \equiv u(+\infty) \geq u_0$. The particle density is assumed to vanish far upstream ($f \rightarrow 0$, $x \rightarrow \infty$), while the only bounded solution downstream is $f(x, p) = f_0(p) \equiv f(0, p)$. We assume Bohm diffusion $\kappa(p) = Kp^2/\sqrt{1+p^2}$. The constant K depends on the $\delta B/B$ level of the magnetohydrodynamic turbulence that scatters particles in pitch angle. However, it can be rescaled out of eq. (1) since we are not interested in the shock structure here.

To include the back-reaction of accelerated particles on the plasma flow the following equations are used in a quasi-stationary acceleration regime: (i) the conservation of the momentum flux in the smooth part of the shock transition (CR-precursor, $x > 0$) $P_C + \rho u^2 = \rho_1 u_1^2$, where P_C is the CR pressure (CRs escape after crossing $p = p_{\max}$), (ii) the continuity equation $\rho u = \rho_1 u_1$, (iii) the Rankine-Hugoniot relations for the sub-shock strength $r_s \equiv u_0/u_2 = (\gamma + 1) / (\gamma - 1 + 2R^{\gamma+1}M^{-2})$ where M is the Mach number at $x = \infty$, the precursor compression $R \equiv u_1/u_0$, and γ is the adiabatic index of the plasma.

These equations self-consistently describe the particle spectrum and flow structure. An efficient solution method is to reduce this system to one integral equation [16]. A key dependent variable is an integral transform of the flow profile $u(x)$ with a kernel suggested by an *exact* (in the limit $M \rightarrow \infty$, $p_{\max} \rightarrow \infty$) asymptotic solution of the system which has the following form

$$f(x, p) = f_0(p) \exp \left[-\frac{q}{3\kappa} \Psi \right], \quad (2)$$

where the flow potential $\Psi = \int_0^x u(x') dx'$ and the spectral index at the sub-shock and downstream $q(p) = -d \ln f_0 / d \ln p$. The integral transform generates the “spectral function” of the flow velocity $U(p)$ instead of the flow velocity $u(x)$ as follows

$$U(p) = \frac{1}{u_1} \int_{0-}^{\infty} \exp \left[-\frac{q(p)}{3\kappa(p)} \Psi \right] du(\Psi), \quad (3)$$

and is related to $q(p)$ as $q(p) = d \ln U / d \ln p + 3/[r_s R U(p)] + 3$. The equation for $U(p)$ is

$$U(t) = \frac{r_s - 1}{R r_s} + \frac{\nu}{K p_0} \int_{t_0}^{t_1} dt' \left[\frac{1}{\kappa(t')} + \frac{q(t')}{\kappa(t) q(t)} \right]^{-1} \times \frac{U(t_0)}{U(t')} \exp \left[-\frac{3}{R r_s} \int_{t_0}^{t'} \frac{dt''}{U(t'')} \right], \quad (4)$$

where $t = \ln p$, $t_{0,1} = \ln p_{0,1}$. The injection parameter $\nu = (4\pi/3)(mc^2/\rho_1 u_1^2) p_0^4 f_0(p_0)$ is related to R :

$$\nu = K p_0 (1 - R^{-1}) \times \left\{ \int_{t_0}^{t_1} dt \kappa(t) \frac{U(t_0)}{U(t)} \exp \left[-\frac{3}{R r_s} \int_{t_0}^t \frac{dt'}{U(t')} \right] \right\}^{-1} \quad (5)$$

Our main goal is to calculate the flux of escaping particles. Since they leave the accelerator through the $p = p_{\max}$ boundary and the solution normalisation is set by the particle distribution at $p = p_{\text{inj}}$ (injection rate), the flux will depend on the entire solution between p_{inj} and p_{\max} . For typical SNR conditions, this interval spans seven orders of magnitude or more and even small errors in the slope along the spectrum will result in a failure of the flux determination. To avoid this, we first compare our analytic solution with a numerical one [8]. The result of the comparison is illustrated in Fig. 1. To compare we substitute the injection rate (i.e., the height of the spectrum at $p = p_{\text{inj}}$) indicated in the Monte Carlo (MC) simulations. To calculate the escaping flux we use the time dependent version of eq. (1) using $g \equiv p^3 f$ in place of f

$$-\frac{\partial g}{\partial t} + \frac{\partial}{\partial x} \left(u g + \kappa(p) \frac{\partial g}{\partial x} \right) = \frac{1}{3} \frac{du}{dx} p \frac{\partial g}{\partial p}, \quad (6)$$

and calculate the temporal variation of the total number of particles in the region $x > 0$ assuming $p_{\max} \simeq \text{const}$ (see [15] for a discussion of this assumption, along with our assumption about

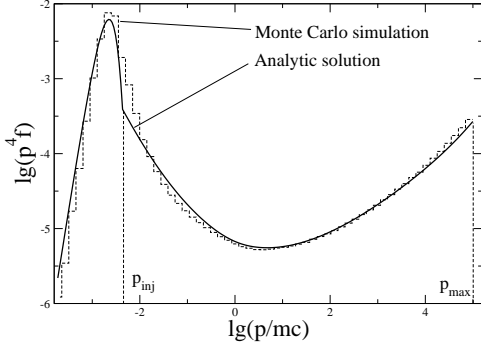


Figure 1: Comparison of our analytic solution with MC simulation [8]. Below p_{inj} , it is a thermal Maxwellian; MC simulation parameters: $M=128$, $p_{max}=10^5$, $\nu \simeq 0.4$.

monoenergetic escape and for further references). Note that $p_{max}(t)$ is adopted in [19, 10]

$$N_{Up} = 4\pi \int_0^\infty dx \int_{p_{inj}}^{p_{max}} g(p, x) dp/p$$

Therefore, from eq. (6) we obtain

$$\begin{aligned} \frac{\partial N_{Up}}{\partial t} = & \frac{4\pi}{3} \int_{0-}^\infty dx \frac{du}{dx} [g(p_{inj}, x) - g(p_{max}, x)] \\ & - 4\pi u_2 \int_{p_{inj}}^{p_{max}} dp \frac{g(p, 0-)}{p}. \end{aligned} \quad (7)$$

In this particle balance equation the term containing $g(p_{inj})$ is simply due to particle injection at $p = p_{inj}$, while the last term is the particle convective flux downstream. The remaining term is the flux of escaping particles

$$\begin{aligned} Q_n &= \frac{4\pi}{3} \int_{0-}^\infty du(x) g(p_{max}, x) \\ &\simeq \frac{4\pi}{3} f_0(p_{max}) p_{max}^3 u_1 U(p_{max}), \end{aligned} \quad (8)$$

where we have used definition of the spectral function $U(p)$ eq. (3), and the solution, eq. (2). Using the plasma number density $n_1 = \rho_1/m_p$ one can obtain the normalised flux as

$$\frac{Q_n}{n_1 u_1} = \nu \frac{u_1^2 p_{max}^3 f_0(p_{max}) U(p_{max})}{c^2 p_{inj}^4 f_0(p_{inj})}.$$

This quantity is plotted in Fig. 2 as a function of compression r . Note that the injection rate obtained from MC simulations corresponds to nearly

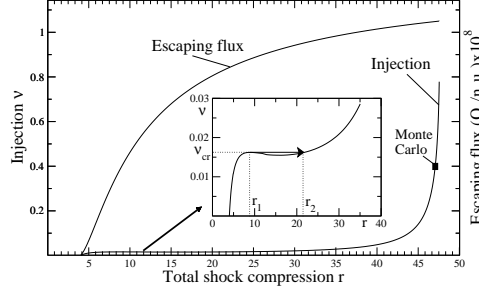


Figure 2: Bifurcation diagram showing injection rate ν (which is actually a control parameter) versus r . The insert shows the region of the “phase transition.” The upper curve shows the particle escaping flux, normalised to the plasma flux far upstream and multiplied by the factor 10^8 , for clarity.

the maximum escaping flux possible, where the function $r(\nu)$ saturates. This saturation is related to the sub-shock smearing, $R^{\gamma+1} \rightarrow M^2$. We believe that the MC method *overestimates* the injection due to the lack of the feedback from particle driven turbulence. It was argued [16] that self-regulation of acceleration, which includes but is not limited to the particle trapping by self-generated waves, leads to a significant reduction of the injection rate which is maintained at nearly the critical level where the shock compression $r(\nu)$ rises sharply, Fig. 2. For the calculations shown in Fig. 2, this approach indeed reduces the injection by an order of magnitude compared to MC results.

Detailed calculations of the escaping flux will be presented elsewhere. Here we note that the normalised flux $Q_n/n_1 u_1$ does not depend strongly on M saturating (when $M \gtrsim 100$) at $Q_n/n_1 u_1 \approx 10^{-5}/p_{max}$ for $u_1=0.005c$. This scaling is the result of energy requirement, since $Q_e = c p_{max} Q_n$ and Q_e is the escaping energy flux which is constrained by the available mechanical energy flux and the equipartition condition. The latter means that for the injection rate close to the critical, about half of the shock energy goes into the CR.

Calculations

Diffuse emission has been detected at the Galactic centre by the HESS [2]. Its intensity correlates with the gas density as traced by the CS emission

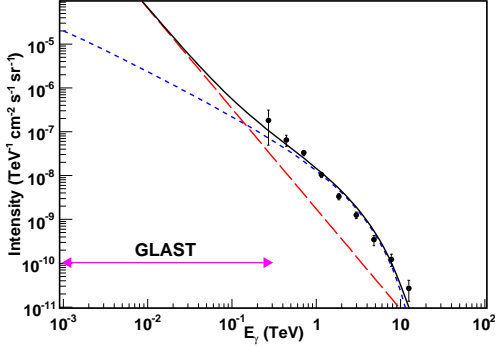


Figure 3: The spectrum of γ -rays from outer (monoenergetic protons of 25 TeV, blue-dots) and inner clouds (power-law with index -2.29 , red-dashes); normalisations are arbitrary. Solid line shows the total spectrum. Data: HESS [2].

up to the >200 pc from the central source, while the SNR shell is about half this size, ~ 100 pc, assuming a SNR age $\tau_{\text{SNR}} \sim 10$ kyr and shock speed 10^4 km s $^{-1}$. Clearly, some part of this emission $\gtrsim 100$ pc may be produced by particles which left the SNR shock $\tau < 1.5$ kyr, if the diffusion coefficient in the ISM $D_{xx}(10 \text{ TeV}) \gtrsim 1 \text{ kpc}^2 \text{ Myr}^{-1}$, i.e. relatively recently $\tau \ll \tau_{\text{SNR}}$.

The HESS data are obtained for the combined emission from all gas clouds in the region. However, the model predicts different VHE γ -ray spectra from clouds at different distances from the SNR. The most distant clouds should exhibit a flatter spectrum with index close to -1 ; closer to the SNR shell the spectrum may steepen and become a regular power-law with index about -2 for clouds located at or inside the shell. To evaluate the feasibility of such scenario, we calculate the spectrum of VHE γ -rays assuming two components: one for the clouds outside of the shell (a monoenergetic ambient spectrum of protons) and another for the clouds inside the shell with a power-law index similar to the central source -2.29 . The spectrum of γ -rays can be evaluated using the scaling approximation [20] as described in [17].

To illustrate the idea, Fig. 3 shows the calculated two-component spectrum from the Galactic centre together with the HESS data. Reasonable agreement with the data can be obtained for a proton injection energy ~ 25 TeV, consistent with the SNR

age of ~ 10 kyr. In the GLAST energy range the spectrum from the outer clouds differs significantly from what is expected for the usual hadronic scenario: it has slope close to -1 . Gabici and Aharonian [10] came to a similar conclusion.

Acknowledgements. We thank Pasquale Blasi and Don Ellison for many useful discussions. I. V. M. thanks NASA APRA grant for partial support. T. A. P. is supported in part by the US Department of Energy. M. A. M and P. H. D. were supported by NASA under grant ATP03-0059-0034 and by the U.S. DOE under Grant No. FG03-88ER53275.

References

- [1] Aharonian, F., *Nature* **416**, 797 (2002).
- [2] Aharonian, F., et al., *Nature* **439**, 695 (2006).
- [3] Aharonian, F., et al., *A&A* **437**, L7 (2005).
- [4] Aharonian, F., et al., *A&A* **449**, 223 (2006).
- [5] Berezhko, E. G., & Völk, H. J., *A&A* **451**, 981 (2006).
- [6] Blandford, R., & Eichler, D., *Phys. Rep.* **154**, 18 (1987).
- [7] Drury, L., *Space Sci. Rev.* **36**, 57 (1983).
- [8] Ellison, D. C., Berezhko, E. G., & Baring, M. G., *ApJ* **540**, 292 (2000).
- [9] Ellison, D. C., & Cassam-Chenaï, G., *ApJ* **632**, 920 (2005).
- [10] Gabici, S., & Aharonian, F., *ApJ* **665**, L131 (2007).
- [11] Jones, F. C., & Ellison, D. C., *Space Sci. Rev.* **58**, 259 (1991).
- [12] Koyama, K., et al., *Nature* **378**, 255 (1995).
- [13] Lazendic, J. S., et al., *ApJ* **602**, 271 (2004).
- [14] Malkov, M. A., Diamond, P. H., & Sagdeev, R. Z., *ApJ* **624**, L37 (2005).
- [15] Malkov, M. A., & Diamond, P. H., *ApJ* **642**, 244 (2006).
- [16] Malkov, M. A., & Drury, L. O., *Rep. Progr. Phys.* **64**, 429 (2001).
- [17] Moskalenko, I. V., & Strong, A. W., *ApJ* **493**, 694 (1998).
- [18] Porter, T. A., Moskalenko, I. V., & Strong, A. W., *ApJ* **648**, L29 (2006).
- [19] Ptuskin, V. S., & Zirakashvili, V. N., *A&A* **429**, 755 (2005).
- [20] Stephens, S. A., & Badhwar, G. D., *Astroph. Space Sci.* **76**, 213 (1981).